

Avascular bone necrosis - How to correctly diagnose or suspect it with X-ray

Poster No.: C-0656
Congress: ECR 2014
Type: Educational Exhibit
Authors: C. M. Oliveira, R. A. Costa, A. Estevao, F. Caseiro Alves; Coimbra/PT
Keywords: Ischemia / Infarction, Diagnostic procedure, Plain radiographic studies, Musculoskeletal bone, Bones
DOI: 10.1594/ecr2014/C-0656

Any information contained in this pdf file is automatically generated from digital material submitted to EPOS by third parties in the form of scientific presentations. References to any names, marks, products, or services of third parties or hypertext links to third-party sites or information are provided solely as a convenience to you and do not in any way constitute or imply ECR's endorsement, sponsorship or recommendation of the third party, information, product or service. ECR is not responsible for the content of these pages and does not make any representations regarding the content or accuracy of material in this file.

As per copyright regulations, any unauthorised use of the material or parts thereof as well as commercial reproduction or multiple distribution by any traditional or electronically based reproduction/publication method is strictly prohibited.

You agree to defend, indemnify, and hold ECR harmless from and against any and all claims, damages, costs, and expenses, including attorneys' fees, arising from or related to your use of these pages.

Please note: Links to movies, ppt slideshows and any other multimedia files are not available in the pdf version of presentations.

www.myESR.org

Learning objectives

1. Explain the pathophysiological mechanisms of avascular bone necrosis (AVN).
2. Illustrate the most common locations where this disease usually develops.
3. Show the different radiographic stages of AVN.
4. Provide examples of rare diseases in which the underlying pathology is AVN.

Background

Avascular necrosis of the bone, also called osteonecrosis, is a phenomenon that involves bone cell death as well as bone destruction, pain and loss of joint function in which the necrotic bone is involved. It can be caused by interruption of arterial inflow, both traumatic and compressive, as well as increased marrow pressure with impeded venous drainage and intraluminal vascular obstruction.

Although there are numerous recognized causes of AVN, there are still many idiopathic cases. The most common causes of AVN include trauma, steroid use, alcoholism and sickle cell disease. There are other minor causes such as Gaucher's disease, radiation or hemophilia.

Although MRI is the most sensitive imaging tool for detection of AVN, this review will focus essentially on conventional radiography findings, as it is frequently the first imaging technique that is used when there is a suspected case of AVN. It is of the utmost importance to know how to read radiographs properly when this disease is suspected.

Pathophysiology of Osteonecrosis

Normal vasculature of the bone

All bones have a blood supply consisting of two components: the nutrient medullary blood supply and the periosteal blood supply. The first one arises from major vascular sources in the limb and consists of small nutrient vascular channels, which enter the bone tiny holes in the cortex and provide a blood supply to the medullary cavity and the inner half of the cortex; the second vascular system consists of small blood vessels arising from the periosteum that enter the cortex and provide a vascular supply to the external half of the cortical structure. They provide the main blood supply to the metaphyseal regions, which serve as the growth zones for children.

Mechanisms for Development of Osteonecrosis

The mechanisms by which blood supply can be interrupted consist of four possible structural or biological disorders:

1. *Mechanical interruption of the blood supply* - Usually results from a fracture of the bone's shaft or a dislocation of a joint, especially in the hip or shoulder. The subchondral region has a low blood supply that can be completely or partially interrupted by an injury, even as limited as a stress fracture or closed trauma.
2. *Vascular thrombosis or embolism*. - If an artery becomes occluded, the portion of the bone that was irrigated by it will become necrotic. Blockages of this sort can result from a thrombus or embolus, dysbarism or abnormally shaped cells (Sickle cell disease).
3. *External injury or pressure on a vascular wall*. - Vascular walls can be temporarily or permanently damaged by radiation, inflammatory disorders, vasculitis, or even excessive pressure by fat or marrow cells.
4. *Venous occlusion (Chandler's disease)*. - If the veins become occluded or compressed, venular pressure may exceed arteriolar pressure in a closed system and as a result, the arterial blood supply can be severely compromised. Even if the arteries are not occluded, this can result in an arteriolar ischemia, leading to cell death.

Clinical Causes of Osteonecrosis

Although the four generic causes described above are the major causes of osteonecrosis, there is a vast number of clinical disorders that have been described as being associated with osteonecrosis. In clinical practice, AVN is most commonly found in the hip. Nonetheless, bones that are extensively covered with articular cartilage are especially vulnerable to AVN after fracture, mainly the proximal pole of the scaphoid, the humeral head and the talar body. Since 2003, AVN of the jaw has been established as a separate pathological entity, related to the use of bisphosphonate therapy. Osteonecrosis can occur in children and the mechanisms for these disorders are poorly understood. Such lesions include Legg-Calve-Perthes, Kienbock's, Freiberg's, Preiser's, and Friedrich's diseases, which may represent forms of Chandler's disease or subtle posttraumatic osteonecrosis.

Findings and procedure details

Imaging

There are four radiographic stages in osteonecrosis. These radiographic findings don't appear until weeks or months after the bone infarct. Keep in mind that magnetic resonance imaging (MRI) is the most sensitive imaging tool for detection of avascular

necrosis, but the cost and time needed to execute those exams prevent a widespread use.

1. In the first stage, there are no radiographic changes despite both MRI and radionuclide bone scans already showing abnormal findings. ([Fig. 1](#) on page 7)
2. In the second stage, the necrotic bone becomes relatively sclerotic, as the vascularized bone surrounding the necrotic bone becomes osteopenic due to hyperemia. ([Fig. 2](#) on page 7)
3. There is bone formation and repair, causing a zone of increased density. In this stage, it is often apparent the "crescent sign" in the subchondral area. In the hip, that sign is best seen on a frog-leg lateral view, but is often discerned on an anteroposterior (AP) view as well. ([Fig. 3](#) on page 8)
4. This subchondral fragmentation causes flattening and deformity of this area of the bone, leading to secondary osteoarthritis, with on-going destruction of both the bone and the joint. ([Fig. 4](#) on page 9 and [Fig. 5](#) on page 10).

We will now show some examples in which the osteonecrosis is present.

Kienböck's disease

Kienböck's disease is a condition where the blood supply to the lunate is interrupted. Damage to the lunate causes a painful, stiff wrist and, over time, can lead to arthritis. The cause of Kienböck's disease is unknown. People with this disease may have experienced some form of trauma to the wrist, such as a fall. This type of trauma can disrupt the blood flow to the lunate. In addition, if the radius and ulna are of different lengths (negative ulnar variance), extra pressure can be put on the lunate during some wrist motions and cause micro-trauma, leading to Kienböck's disease. There are four stages of this disease:

1. The symptoms are similar to those of a wrist sprain. Although the blood supply to the lunate has been disrupted, x-rays may still appear normal or suggest a possible fracture. An MRI scan can better detect blood flow and is helpful in making the diagnosis in this early stage. ([Fig. 6](#) on page 11)
2. The lunate bone becomes sclerotic due to the lack of blood supply. ([Fig. 7](#) on page 12)
3. The dead lunate bone begins to collapse and break into pieces. As the bone begins to break apart, the surrounding bones may begin to shift position. During this stage, patients typically experience increasing pain, weakness in gripping, and limited wrist motion. ([Fig. 8](#) on page 14)
4. If the condition progresses to Stage 4, the surfaces of the bones surrounding the lunate also deteriorate and the wrist may become arthritic.

Osteonecrosis of the talus

The talus is the second largest of the tarsal bones and has a unique structure designed to channel and distribute body weight. Approximately 60% of its surface is covered by articular cartilage, and there are no muscular or tendinous attachments to this bone. Consequently, only a limited area of penetrable bone is available for vascular perforation and predispose the talus to osteonecrosis when its vascular supply is disturbed.

Although no specific radiographic classification system exists, osteonecrosis of the talus exhibits a characteristic radiographic pattern. It usually appears as an area of increased opacity or sclerosis in the talar dome that may extend into the talar body, with possible collapse of the articular surface and, in severe cases, fragmentation of the talar dome and body.

At initial radiography, necrotic bone and the surrounding viable bone are equal in opacity, and early AVN can be missed. As time passes and hyperemia results, healthy bone is resorbed and subsequently becomes osteopenic. At this point, radiographic evidence of talar AVN becomes apparent. ([Fig. 9](#) on page 16)

The opacity of necrotic bone continues to increase and accounts for the typical sclerotic picture seen in AVN of the talus. MRI is the most sensitive technique for detecting osteonecrosis of the talus, especially in the early stages. In addition, MRI can be used when there is a high clinical suspicion for AVN in the setting of normal radiographic findings. CT scans also reveal characteristic talar AVN patterns and can be used to confirm radiographic findings. Despite the availability of cross-sectional imaging, however, conventional radiography remains the mainstay of the diagnosis and temporal observation of talar AVN. [Fig. 10](#) on page 16 and [Fig. 11](#) on page 17 provide another examples of osteonecrosis of the talus.

Freiberg's disease

Freiberg's disease is a disorder affecting the metatarsal head (usually the second or third metatarsal head) and is characterized by collapse of the subchondral bone, osteonecrosis, and cartilaginous fissures. It is believed that the disease is probably multifactorial. A traumatic event or vascular compromise are the most popular theories. High-heeled shoes have been implicated as a causative factor. Patients may present with pain and limited motion, although symptoms may not begin until degenerative arthrosis has developed. In an early state, radiographs show flattening and cystic lesions of the affected metatarsal head ([Fig. 12](#) on page 18) as well as widening of the metatarsophalangeal joint; if the disease progresses, osteochondral fragments become visible, with increased cortical thickening.

Legg-Calvé-Perthes disease

Legg-Calvé-Perthes disease (LCPD) consists in a form of idiopathic avascular necrosis of the growing femoral epiphysis seen in children, usually affecting those with 4-8 years. The most frequent presenting feature is pain with or without a limp. In 10-12 % of cases both hips are involved.

The radiographic findings are those of AVN. In the early stages of the disease, where is an asymmetrical femoral epiphyseal size with apparent increased density of the femoral head epiphysis and widening of the medial joint space (stage 1 - [Fig. 13](#) on page 21). During the course of the disease, the femoral head eventually begins to fragment (stage 2 - [Fig. 14](#) on page 21), with subchondral lucency (crescent sign). In the late stages of the disease, there is widening and flattening of the femoral head deformity ([Fig. 15](#) on page 21) .

The presence of metaphyseal involvement not only increases the likelihood of femoral neck deformity, but also make early physeal closure resulting in leg length disparity.

MRI is gaining an increasing role in diagnosing this disease before the onset of x-ray findings, as well as assessing the extent of cartilaginous involvement and joint stability.

Osteonecrosis after fracture

Although virtually any bone that suffers a fracture and loses its vascular supply can become necrotic and present itself in radiographs as a sclerotic bone, we will show a particular example:

Osteonecrosis of the proximal end of the scaphoid after a fracture.

Scaphoid fractures are common and can sometimes be difficult to diagnose resulting in significant functional impairment. They account for 70-80% of all carpal bone fractures, usually after falling on an outstretched hand with resultant hyper-extension of the wrist or purely compressive force.

Plain radiographs of the wrist, including dedicated scaphoid views should be acquired whenever a scaphoid fracture is suspected. It should however be noted that initial radiograph can miss from 5-20% of fractures in the acute setting. The scaphoid blood supply is different from the expected - arterial flow to the scaphoid enters via the distal pole and travels to the proximal pole in a retrograde fashion. This blood supply is tenuous, increasing the risk of non-union, particularly with fractures at the wrist and proximal end. If AVN develops the first sign will be slight sclerosis of the proximal pole of the scaphoid ([Fig. 16](#) on page 19). This can be on account of the rest of the wrist undergoing demineralisation due to immobilisation, whereas the proximal portion being bereft of

blood supply retains its calcium. With time the proximal part undergoes osteonecrosis, becomes increasingly sclerotic and become fragmented.

Images for this section:

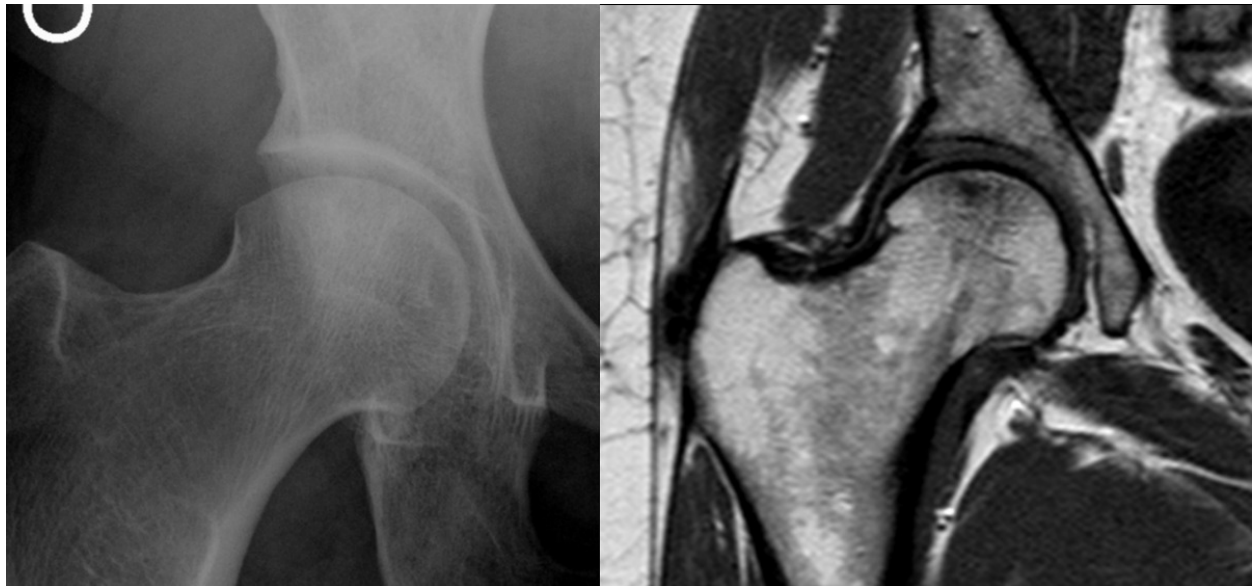


Fig. 1: Stage 1 - Plain radiograph and T1-weighted MRI image of the right hip. There are no abnormal findings in the left image, although there are already some signs of osteonecrosis on the femoral head on the MRI.



Fig. 2: Stage 2 - This radiograph shows some sclerosis of the femoral head, mainly in its superior portion.

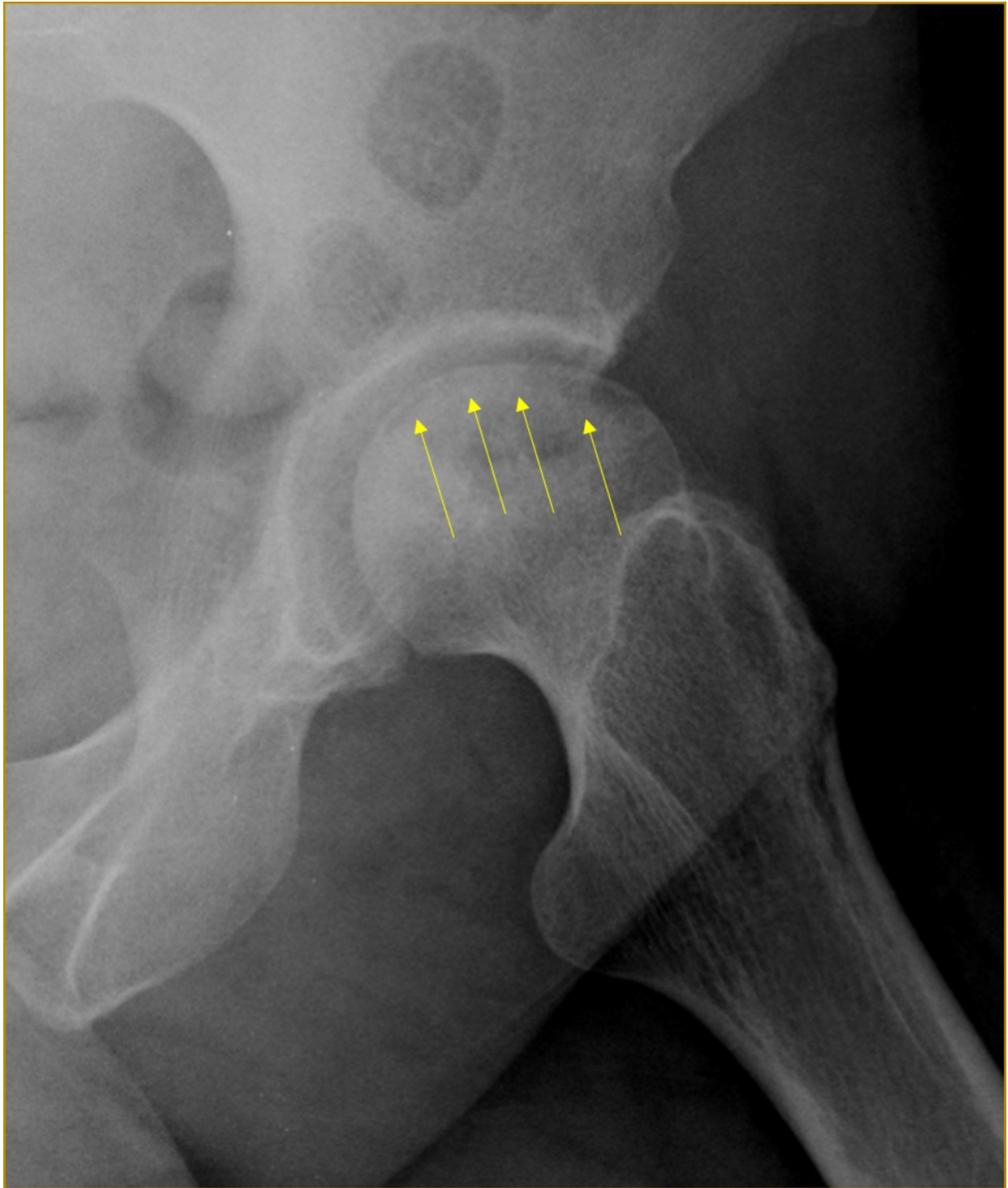


Fig. 3: Crescent sign - This radiograph show the crescent sign (radiolucency in shape of a band in a subchondral position). This sign is virtually pathognomic of AVN, despite not being always present. It usually appears when the bone is about to fracture.



Fig. 4: Stage 4 - There is already some degree of deformation and flattening of the femoral head, leading to secondary osteoarthritis.



Fig. 5: Osteonecrosis of the humeral head in the last stage, with visible bone destruction and fragmentation.



Fig. 6: Kienböck's disease - T1-weighted MRI image of the right wrist, showing a devitalized lunate bone.



Fig. 7: Kienböck's disease stage 2 - This radiograph shows a sclerotic lunate due to the lack of blood supply. Compare with the rest of the carpal bones.

D



Fig. 8: Kienböck's disease stage 3 - The dead lunate bone begins to show signs of collapse.



Fig. 9: Osteonecrosis of the talus - There is already some degree of sclerosis on the dome of the talus, on its medial portion (seen on the left and middle pictures). Although that AVN site is pretty obvious on the T1-weighted image we provide (right picture), it could be overlooked by the untrained eye in the plain radiographs.



Fig. 10: Osteonecrosis of the talus - Plain radiograph and T1-weighted MRI image that gives another example of a necrotic spot on the talar dome, in its medial portion.

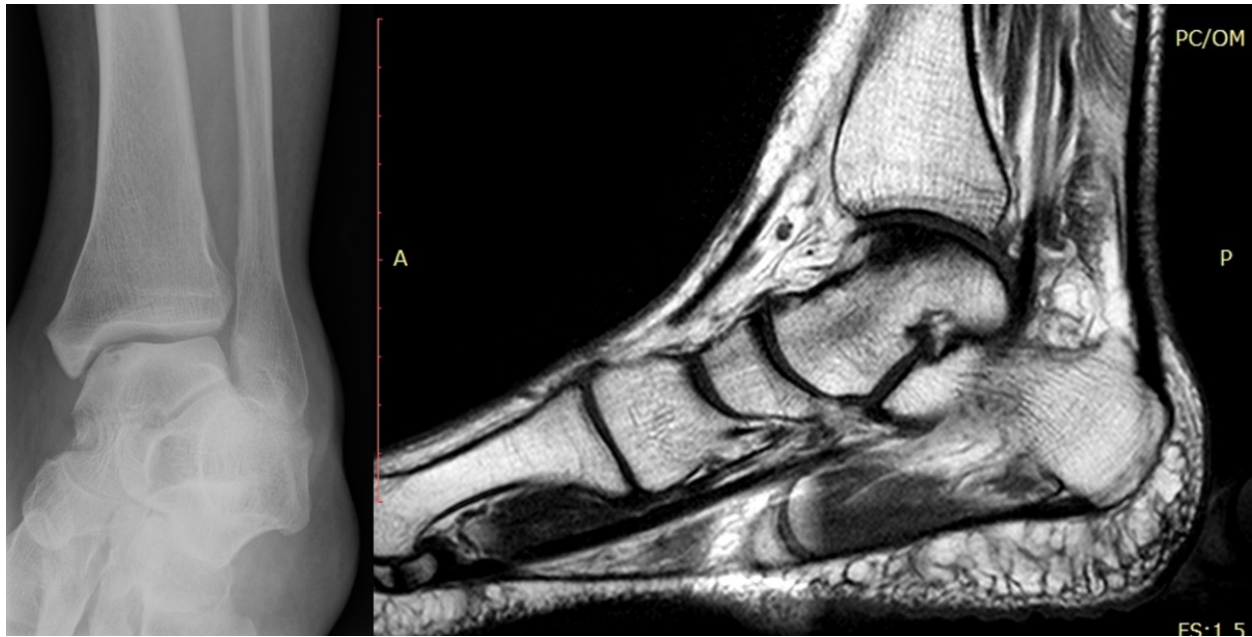


Fig. 11: Osteonecrosis of the talus - Plain radiograph and T1-weighted MRI image that give yet another example of a necrotic spot on the talar dome, in its medial portion. Note the subchondral lucency in the radiograph, similar to the crescent sign already described previously.



Fig. 12: Freiberg's disease - In the right foot, there is deformity, enlargement and some subchondral cysts in the second metatarsal head. Compare with the left second metatarsal head, which is not affected by the disease.



Fig. 16: Osteonecrosis of the scaphoid - Plain radiograph of the carpal bones showing a sclerotic proximal pole of the scaphoid (yellow arrows), following a complete fracture through the scaphoid waist with blood supply interruption.

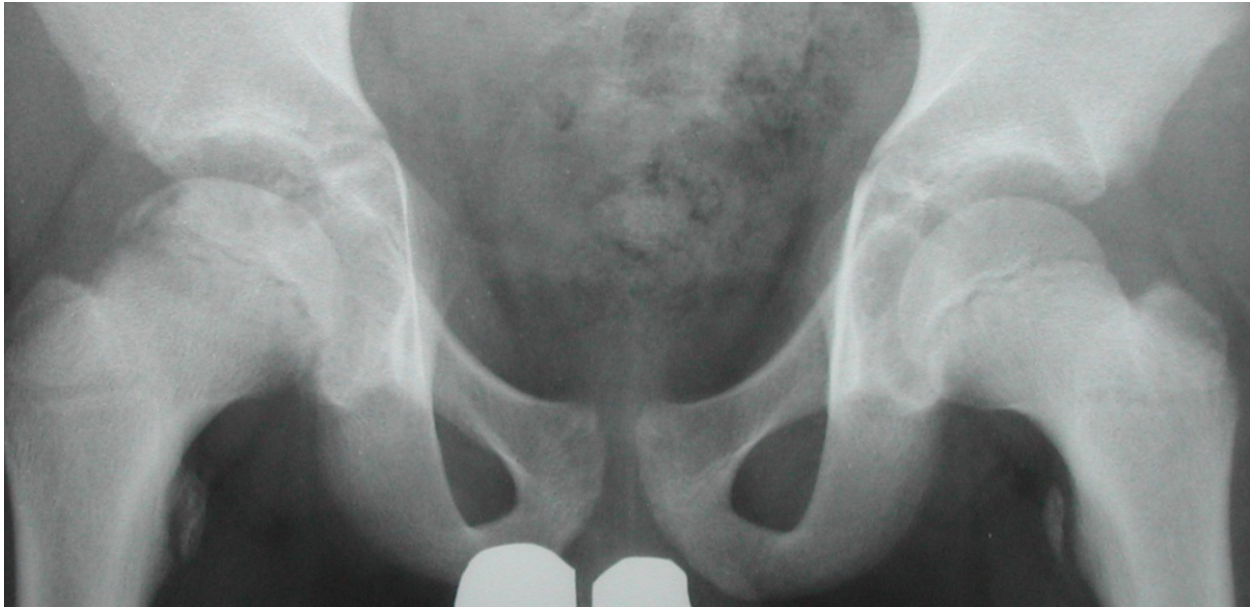


Fig. 13: Legg-Calvé-Perthes' disease stage 1 - There is an assymetrical femoral epiphyseal size with apparent increased density of the right femoral head epiphysis and widening of the medial joint space.



Fig. 14: Legg-Calvé-Perthes' disease stage 2 - The left femoral head is fragmented. Sometimes, it is possible to see a subchondral lucency (crescent sign), in close resemblance of the adult hip AVN.

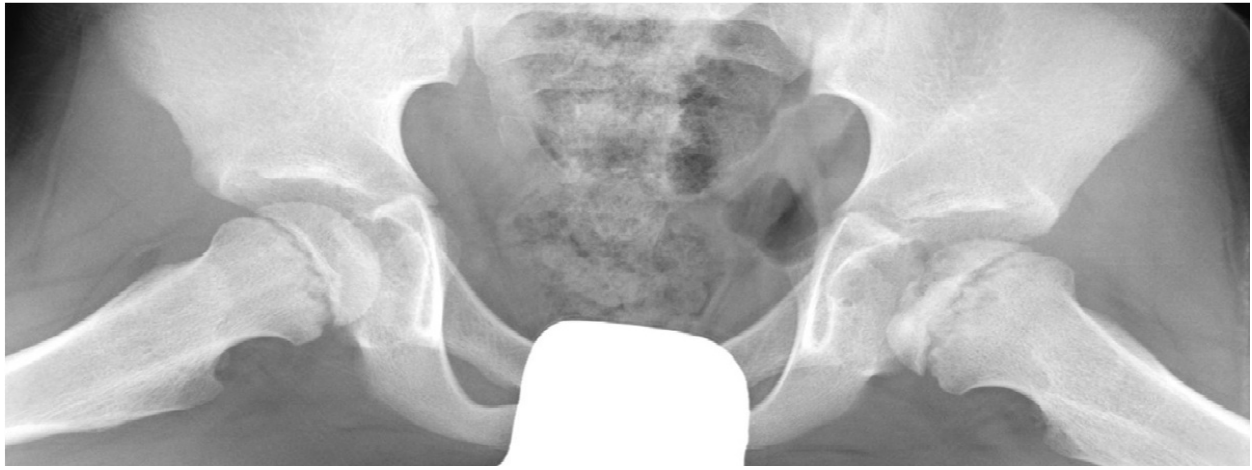


Fig. 15: Legg-Calvé-Perthes' disease stage 4 - There is widening and flattening of the left femoral head. If not treated, there can be length disparities between the two limbs.

Conclusion

Although MRI is the gold-standard to diagnose avascular bone disease nowadays, the x-ray still plays an important role in this process, as it is usually the first imaging technique used when suspicion arises. Some of the radiographic findings are pathognomonic, providing an earlier diagnosis and a better and faster treatment to the patient.

Personal information

References

Greenspan, A.; *Orthopedic Imaging - A Practical Approach*; 5th Edition; Lippincott Williams & Wilkins, 2011

Brant, WE; Helms, C.; *Fundamentals of Diagnostic Radiology*; 4th Edition; Lippincott Williams & Wilkins, 2012

Pearce DH, Mongiardi CN et al; *Avascular necrosis of the talus: a pictorial essay*; Radiographics. 2005 Mar-Apr;25(2):399-410.

Jaramillo D, Galen TA, Winalski CS et al. *Legg-Calvé-Perthes disease: MR imaging evaluation during manual positioning of the hip--comparison with conventional arthrography*. Radiology. 1999;212 (2): 519-25

Ashman CJ, Klecker RJ, Yu JS. *Forefoot pain involving the metatarsal region: differential diagnosis with MR imaging*. Radiographics. 21 (6): 1425-40.